



Published in final edited form as:

Environ Sci Technol. 2011 August 1; 45(15): 6483–6490. doi:10.1021/es201379a.

A Personal Nanoparticle Respiratory Deposition (NRD) Sampler

Lorenzo G. Cena, T. Renée Anthony, and Thomas M. Peters

Department of Occupational and Environmental Health, The University of Iowa, Iowa City, IA

Abstract

A lightweight (60 g), personal nanoparticle respiratory deposition (NRD) sampler was developed to selectively collect particles smaller than 300 nm similar to their typical deposition in the respiratory tract. The sampler operates at 2.5 Lpm and consists of a respirable cyclone fitted with an impactor and a diffusion stage containing mesh screens. The cut-point diameter of the impactor was determined to be 300 nm with a sharpness $\sigma = 1.53$. The diffusion stage screens collect particles with an efficiency that matches the deposition efficiency of particles smaller than 300 nm in the respiratory tract. Impactor separation performance was unaffected by loading at typical workplace levels (p -value = 0.26). With chemical analysis of the diffusion media, the NRD sampler can be used to directly assess exposures to nanoparticles of a specific composition apart from other airborne particles. The pressure drop of the NRD sampler is sufficiently low to permit its operation with conventional, belt-mounted sampling pumps.

Introduction

Workers produce and handle engineered nanomaterials in substantial quantities in the manufacture of hundreds of commercial products.(1) Exposure through inhalation of these materials is a primary concern for worker health and safety because of the sensitivity of the respiratory system.(2) The airborne nanoparticle component (≈ 100 nm) is of particular concern because nanoparticles can elicit substantially greater toxic effects than larger particles of the same composition.(3, 4) Moreover, nanoparticles may translocate from the respiratory tract to other organs and the bloodstream.(5, 6) The National Institute for Occupational Safety and Health (NIOSH) has proposed draft guidelines for ultrafine titanium dioxide, which includes recommended exposure limits and an exposure assessment method.(7) The proposed exposure assessment method relies on traditional 8 h, filter-based, personal respirable sampling.(7)

Size-selective samplers are used to collect particles with efficiencies that represent how particles enter into or deposit within the respiratory system. Respirable samplers are used to collect particles with efficiencies that approximate the fraction of aerosol that, once inhaled, can penetrate into the gas-exchange region of the respiratory tract.(8) These samplers are designed to match the respirable particulate matter sampling criterion, which defines collection efficiency of particles as 50% for 4 μ m particles and 100% for particles smaller than 1 μ m.(9) By this definition, respirable samplers must prevent the collection of larger particles (>10 μ m) that may exist in the environment while selectively sampling only these smaller particles at the specified collection efficiencies. However, when aerosols include both nanoparticles and respirable particles, the mass measured from a sample collected using

a respirable sampler will often be dominated by the larger, non-nanoparticles. Hence, in many occupational environments, where nanoparticles and respirable particles coexist, the respirable sampler has limited usefulness in quantifying nanoparticle exposures.

To overcome this problem for assessing titanium dioxide nanoparticle exposures, NIOSH recommends analysis by electron microscopy with energy dispersive X-ray spectroscopy to characterize the size and composition of nanoparticles apart from the larger particles collected with a respirable sampler.(7) However, there are no standard methods for this analysis, and electron microscopy is particularly expensive (>300 USD per sample) compared to bulk chemical analysis methods (~30 USD per sample).

A personal sampling method that removes larger respirable particles and only collects nanoparticles would streamline exposure assessments. An ideal sampler would be portable, allow placement within the breathing zone of a worker and collect nanoparticles in a way that mimics their respiratory deposition.(10) By capturing only nanoparticles on the sampling media, cost-efficient bulk analysis techniques (e.g., inductively coupled plasma mass spectrometry) could then be used to estimate the amount of deposited nanomaterials.

Wire mesh screens have been used successfully to preferentially collect nanoparticles.(11) The Brownian motion of particles smaller than 300 nm enhances their deposition onto the surface of the wires by diffusion.(12) Stainless steel screens have typically been used, although they are incompatible with bulk analyses techniques that require dissolution of the collection media.(13) Gorbunov et al.(14) developed a size-selective sampler that uses an impactor to remove large particles and nylon mesh screens to collect nanoparticles. They analyzed these nanoparticles by treating the nylon mesh screens in *aqua regia* and subjecting them to microwave digestion. While their sampler provides a method for separating and analyzing nanoparticles from other aerosol components, its large size limits this sampler to area sampling and does not collect particles with physiological relevance.

This work presents the development of a personal nanoparticle respiratory deposition (NRD) sampler that was designed to be capable for deployment as a full-shift, personal sampler that selectively collects nanoparticles apart from larger particles in a workplace atmosphere. Rather than attempting to collect nanoparticles with 100% efficiency, the sampler was designed to collect nanoparticles with efficiency matching how they deposit in the respiratory tract to provide a physiologic relevance to sampler's performance. Consequently, the NRD sampler is fundamentally different from commonly used samplers (e.g., respirable and inhalable samplers) that are based on penetration of particles to different regions of the respiratory system.(15) A new sampling criterion—nanoparticulate matter (NPM)—was first devised to provide the target collection efficiency, by particle size, for the sampler. The NRD sampler presented here was developed by incorporating a respirable sampler (to eliminate particles larger than 10 μm), an impaction plate (to further remove particles larger than 300 nm) and a deposition stage where the remaining nanoparticles deposit onto nylon mesh screens with collection efficiency to match this target sampling criterion. Subsequent chemical analysis of the nanoparticles deposited on the collection media of the NRD sampler allows for characterization of nanoparticles apart from larger background particles.

Materials and Methods

Development of a Target Size Selection Curve

Particle deposition in all regions of the respiratory tract is shown as the dashed line in Figure 1. Deposition of particles measured experimentally under a wide variety of conditions (16–18) generally follows the respiratory deposition curve for the average adult under light exercise and nose-breathing conditions presented by the International Commission on Radiological Protection (ICRP). (19) For this reason, the ICRP curve was used to develop the NPM sampling criterion. The region of interest for the NPM curve was all particles smaller than 300 nm, the minimum deposition for submicrometer particles.

We have defined NPM fraction, for a given particle diameter, as the fraction of those particles smaller than 300 nm that, when inhaled, can deposit in the respiratory system. Therefore, the NPM fraction is a subset of the inhalable particulate matter (IPM) collection efficiency, defined as

$$\text{IPM}(d) = 0.5[1 + \exp(-0.06d)] \quad \text{for } (0 < d \leq 100 \mu\text{m}) \quad (1)$$

where d is the particle diameter in μm . (9) The collection efficiency for NPM is given by

$$\text{NPM}(d) = \text{IPM}(d)[1 - F(x)] \quad (2)$$

where $F(x)$ is the cumulative probability density function of the standardized normal variable x ,

$$x = \frac{\ln(d/\Gamma)}{\ln(\Sigma)} \quad (3)$$

with $\Gamma = 0.04 \mu\text{m}$ (40 nm), and $\Sigma = 3.9$. The mathematical form for this criterion is the same as that used for the thoracic and respirable criteria. (9) The value for Γ represents the particle size associated with 50% deposition, or d_{50} cutoff diameter. This value was selected as the particle size smaller than 300 nm associated with 50% deposition as defined by the ICRP curve. Examining Figure 1, we find that in this region $d_{50} = 40 \text{ nm}$. The value for Σ was fitted by minimizing the sum of squares error between the ICRP total deposition curve and the NPM equation for particles smaller than 300 nm. This minimization was carried out in an MS Excel (Microsoft Corp., Redmond, WA) spreadsheet using the solver function.

The resulting NPM sampling criterion is shown by the solid line in Figure 1. This criterion provided a rational target for the development of the NRD sampler and ties its performance to the physiologically relevant fractional deposition of nanoparticles in all regions of the respiratory tract. The shallow shape of the collection efficiency curve matched the collection efficiency performance form associated with diffusion techniques (rather than the sharp curve associated with impaction). This shallow target curve allowed the sampler to rely on diffusion-based collection with a pressure drop compatible with conventional occupational hygiene belt-mounted sampling pumps.

Description of the NRD Sampler

The NRD sampler consists of three primary components assembled in series: a 25 mm respirable aluminum cyclone (model 225-01-01, SKC Inc., Eighty Four, PA), an impaction stage and a diffusion stage (Figure 2). Air is drawn through the cyclone, which removes particles larger than the respirable sampler criterion and transports the respirable fraction to the impaction stage, where particles larger than 300 nm are removed. In the diffusion stage, the remaining airborne nanoparticles diffuse to and are collected onto eight hydrophilic nylon mesh screens with 11 μm pore size and 6% porosity (model NY1102500, Millipore Inc., Billerica, MA) with an efficiency closely matching the NPM sampling criterion.

The sampler is lightweight (~60 g), fits in a standard lapel mount (model 225-1, SKC Inc., Eighty Four, PA) and operates at an airflow rate (Q) of 2.5 Lpm with a pressure drop of 3.54 kPa (14.2 in. H_2O). The sampler can be used with a commercially available belt-mounted sampling pump for the duration of a work-shift (e.g., AirCheck 2000, SKC Inc., Eighty Four, PA).

The impaction stage was designed following Marple and Willeke (1976) impactor design procedures to achieve a d_{50} of approximately 300 nm at a flow rate $Q = 2.5$ Lpm. The initial design parameters included the selection of jet width (W) and number (n) to achieve a Reynolds number $500 < Re < 3000$. This stage consists of three round acceleration nozzles having a width W and throat length L and an impaction plate at a distance S from the nozzles. The impaction plate requires the application of a thin layer of vacuum grease prior to operation. The final design parameters are presented in Table 1 and were calculated assuming temperature $T = 20^\circ\text{C}$, pressure $P = 98.6$ kPa, aerosol particle density (sodium chloride) $\rho_p = 2200$ kg/m^3 , air density $\rho_g = 1.2$ kg/m^3 and air viscosity $\mu = 1.81 \times 10^{-5}$ Pa s.

Filtration theory from Cheng et al.,(20) validated and modified for use with nylon mesh screens in our laboratory tests, was used to determine the number and mesh size of diffusion screens necessary to match the NPM sampling criterion. The diffusion screens are tightly held in place in the diffusion stage by an aluminum ring with three spokes. Tests of the collection efficiencies of the impactor, both clean and preloaded, and the mesh screen diffusion collector were performed in series.

Evaluation of the Impactor Performance

The experimental setup used to evaluate the impaction stage is included as Supporting Information (Figure S1). A three-jet Collision nebulizer (BGI, Waltham, MA) was used to aerosolize a 16% (by volume) aqueous sodium chloride (Fisher Scientific, lot no. 028258) solution. The resulting polydisperse aerosol was fed into a dilution chamber, mixed with clean, dry air, and passed through a charge neutralizer (model 3054, TSI Inc., Shoreview, MN) and a diffusion dryer (model 3062, TSI Inc., Shoreview, MN). The aerosol was then passed into a 0.002 m^3 glass chamber, through the impactor stage and into a second identical glass chamber.

The particle number concentration by size was measured alternately from within the glass chamber upstream (C_{in}) and from within that downstream (C_{out}) of the impactor. Sampling probes and tube lengths were carefully matched so that particle losses upstream and

downstream the impactor would be equal. A scanning mobility particle sizer (SMPS, model 3080, TSI Inc., Shoreview, MN; airflow = 0.3 Lpm) was used to count particles from 15 to 500 nm, and an aerodynamic particle sizer (APS, model 3321, TSI Inc. Shoreview, MN) was used to count particles from 0.5 to 2 μm . For the APS data, each particle size interval was converted from aerodynamic diameter to mobility equivalent diameter following Peters et al. (21) The APS inlet was modified so that the 1 Lpm sample entered directly into the aerosol inlet at 1 Lpm and the 4 Lpm sheath air, which is internally filtered, was left open to room air. A mass flow controller (model GFC37, Aalborg Instruments & Controls Inc., New York, NY) was used to maintain a constant flow rate of 2.5 Lpm drawn through the impactor with a vacuum pump (model 4F740A, Gast Manufacturing Inc., Benton Harbor, MI). The alternating of measurements upstream and downstream of the impactor was repeated at least three times. A differential pressure gauge (Magnehelic 2020, Dwyer Instruments Inc., Michigan City, IN) was connected to each glass chamber to measure the pressure drop across the impactor stage.

The collection efficiency (E) of the impactor stage for a given particle size (i) was calculated as: $E_i = 1 - C_{\text{out},i}/C_{\text{in},i}$. The collection efficiency data were fitted with a logistic sigmoidal algorithm (OriginPro v8.5, OriginLab Corporation, Northampton, MA) of the form

$$E = a_2 + \frac{a_1 - a_2}{1 + \left(\frac{d}{x_0}\right)^p} \quad (4)$$

where a_1 , a_2 , x_0 , and p are the coefficients determined by the algorithm. The sigmoidal algorithm allowed accurate estimation of the d_{50} , d_{84} , and d_{16} of the impactor stage, which correspond respectively with the 50%, 84%, and 16% collection efficiencies of the impactor. The sharpness (σ) of the collection efficiency curve was calculated following Hinds(22) as

$$\sigma = \sqrt{\frac{d_{84}}{d_{16}}} \quad (5)$$

Evaluation of Impactor Performance after Loading

The performance of the impactor after being loaded with particles was evaluated using the experimental setup shown in the Supporting Information (Figure S2). An aerosol composed of fine test dust (batch no. 1569, AC Spark Plug Company, Flint, MI) with 10- μm volume median diameter was generated using a fluidized bed aerosol generator (model 3400, TSI Inc., Shoreview, MN) and injected into a 0.02 m^3 sampling chamber. The aerosol in the chamber was sampled simultaneously with two samplers: (1) the NRD respirable cyclone with the impactor stage downstream; and (2) the NRD respirable cyclone with a 37 mm filter cassette containing a Teflo filter (P/N 225-1709, SKC, Inc., Eighty Four, PA) with a support pad downstream. The filter was weighed before and after each test using a microbalance (model MT5, ISO 9001, Mettler-Toledo Inc., Columbus, OH) to determine the mass concentration of dust passing to the impactor.

Two loading levels were targeted to simulate sampling in an environment with 3 mg/m^3 passing the cyclone to the impactor for 4 h ($12 \text{ mg/m}^3 \times \text{h}$) and 8 h ($24 \text{ mg/m}^3 \times \text{h}$). These values represent worst-case loading of the impactor at the threshold limit value established by the American Conference of Governmental Industrial Hygienists for respirable particles not otherwise specified over times relevant to workplace sampling. Actual loading levels measured from the filter sampler for the targeted 4 and 8 h loading scenarios were, respectively, $13.6 \text{ mg/m}^3 \times \text{h}$, and $21.5 \text{ mg/m}^3 \times \text{h}$.

After loading, the impaction stage was separated from the cyclone and placed in the previously described impaction stage evaluation setup (see the Supporting Information). The sampler's efficiency, now with preloaded impaction stages, was again tested with sodium chloride aerosol. The collection efficiency was measured in triplicate following the same procedures outlined above in the impaction stage evaluation. Each loading and collection efficiency measurement was repeated twice and the impaction substrate was cleaned and new grease (High Vacuum Grease, Dow Corning Corporation, Midlan, MI) was applied prior to each loading replicate.

Two-way analysis of variance (ANOVA) was performed (Minitab, Minitab Inc., State College, PA) on efficiency versus loading and particle size to determine whether the collection efficiency was significantly affected by loading of the impaction substrate ($p < 0.05$). The loading levels used in the ANOVA were no previous loading, $13.6 \text{ mg/m}^3 \times \text{h}$, and $21.5 \text{ mg/m}^3 \times \text{h}$.

Effective Deposition to the Screens of the NRD Sampler

The experimental setup used to measure the effective deposition on the diffusion stage of the NRD sampler is included as Supporting Information (Figure S3). Deposition was computed for monodispersed aerosols with mean particle diameters of 20, 40, 100, 200, and 500 nm. To generate seed aerosol for 20 nm tests, an electrospray aerosol generator (model 3480, TSI Inc., Shoreview, MN) was used to aerosolize a 0.01% (by volume) solution of ammonium fluorescein ($\text{C}_{20}\text{H}_{12}\text{O}_5$, Acros Organics, lot no. A0206621001) in 0.01 N ammonium hydroxide (NH_4OH). A three-jet collision-type nebulizer (BGI, Waltham, MA) was used to nebulize an ammonium fluorescein solution of 0.03% by volume for the 40, 100, and 200 nm tests and 0.15% by volume for the 500 nm tests. The aerosol was fed into a dilution chamber, mixed with clean dry air and passed through an electrostatic classifier model 3071, TSI Inc., Shoreview, MN). Because of the difficulty to produce substantial concentrations of small (20 nm) fluorescein particles, the dilution chamber was removed during the generation of the 20 nm aerosol with the electrospray aerosol generator. The resulting monodisperse aerosol was neutralized (model 3054, TSI Inc., Shoreview, MN) and dried (model 3062, TSI Inc., Shoreview, MN) before entering a 0.02 m^3 sampling chamber. An SMPS (model 5.4 Grimm Technology, Douglasville, GA) was used to verify particle size and number concentration in the sampling chamber.

The fully assembled NRD sampler (25 mm aluminum cyclone with impaction stage and diffusion stage containing 8 nylon mesh screens) and a 37 mm open-face filter cassette containing two Durapore membrane filters with a support pad (P/N DVPP04700, Millipore, Billerica, MA) were placed inside the sampling chamber. Two separate vacuum pumps

(Omni-5, BGI, Waltham, MA) were used to draw an airflow of 2.5 Lpm through each sampler. The vacuum pumps were calibrated with a mass flow meter (model 4146, TSI Inc., Shoreview, MN) prior to each test. Particles were collected for a period of time ranging between 75 min for the 500 nm particles and 12 h for the 20 nm particles to ensure collection of a sufficient quantity of fluorescent material to detect particles on the collection substrate of the diffusion stage.

The amount of fluorescent material deposited on the screens of the diffusion stage and on the filter of the open-face cassette was determined following the protocol outlined by Tolocka et al.(23) Both substrates were immersed in 4 mL of 0.01 N NH₄OH and sonicated (Solid State/Ultrasonic FS-14, Fisher Scientific Inc., Pittsburgh, PA) for 10 min. The mass concentration of fluorometric material in the recovered solution was determined using a fluorometer (Modulus 9200, Turner BioSystems, Sunnyvale, CA). The deposition efficiency (D_D) of particles on the diffusion stage was calculated as $D_D = M_D/M_F$, where M_D is the mass concentration of fluorometric material deposited on the diffusion substrate and M_F is that deposited on the filter of the open-face cassette. These deposition and recovery procedures were repeated three times for each particle size, and new nylon mesh screens and filters were used for each repetition. Mean deposition efficiency of these repetitions was compared to the NPM curve and assessed for fit.

Results and Discussion

Evaluation of the Impactor Performance

The collection efficiency curve of the impaction stage is shown in Figure 3, and the physical characteristics and parameters of the stage are reported in Table 1. The minimum collection efficiency ($8\% \pm 3\%$) was observed for particles with a diameter near 100 nm. For particles progressively smaller than this minimum value, collection efficiency gradually increased to $26\% (\pm 7\%)$ for 15 nm particles. This increase in efficiency is attributed to diffusion losses that may occur throughout the impactor stage. A similar increase in efficiency due to diffusion was observed in the smallest stages of a recently developed, high flow rate (40 Lpm), portable nanosampler consisting of four impaction stages and an impaction filter.(24) For particles larger than 100 nm, the collection efficiency of the NRD sampler impaction stage rapidly increased to $96\% (\pm 6\%)$ for 550 nm particles. Particles in this size range carry sufficient inertia to impact upon the greased impaction plate where they were trapped.

The characteristic cutoff diameter (d_{50}) of the impactor stage was measured to be 295 nm, and the geometric standard deviation (σ) or collection efficiency sharpness was 1.53. This curve is sufficiently sharp to remove particles larger than the target cutoff diameter (300 nm) from the airstream. The square root of Stokes number at the 50% collection efficiency was 0.32 and the pressure drop (P) across the stage was 2.49 kPa. The Reynolds number of the impactor nozzles was 2212, within the desired range of $500 < Re < 3000$, where the efficiency curve is at its sharpest.(25)

Impactors have been developed that offer cutoff diameters similar to that of the NRD impaction stage.(26–29) For example, low pressure impactors operate at pressures substantially lower than atmospheric to reduce drag forces and allow collection of particles

as small as 50 nm.(30) Micro orifice impactors employ up to a few thousand small (40–200 μm) round nozzles to achieve smaller cutoff diameters. These impactors achieve sharper collection efficiency curves ($\sigma = 1.2$) than the impaction stage of the NRD sampler, however, they require rather large pumps to achieve high flow rates and low pressures, making them less portable.(25) In contrast, commercially available belt-mounted pumps are capable of handling the pressure drop imparted by the impaction stage of the NRD sampler.

Misra et al.(31) developed a personal cascade impactor sampler that consists of four impaction stages and operates at a flow rate of 9 Lpm with a pressure drop of 2.7 kPa (11 in. of H_2O), a pressure drop compatible with a somewhat larger than normal belt-mounted vacuum pump. Similarly to the NRD impaction stage, the final stage of their personal cascade impactor achieves a cutoff diameter of 250 nm with collection efficiency sharpness ranging between 1.28 and 1.53 depending on the collection substrate employed in the stage. (31)

Evaluation of Impactor Performance after Loading

The results of the loading tests performed on the impaction stage are summarized in Table 2. When compared to tests with no prior loading, the effect of particle loading on collection efficiency was negligible, as the means ± 1 standard deviation overlap for all values in Table 2. The results of the two-way ANOVA confirmed that there is not a significant difference in efficiency between loadings (p -value = 0.257). The p -value for the interaction term between particle size and loading was close to significant (p -value = 0.063) at a 5% alpha level, indicating that with different loadings the efficiency varies at different particle sizes. The greatest reduction of the impactor's collection efficiency was observed at 15 nm, the smallest particle size tested, where efficiency after loading experienced the greatest decrease from $E = 0.26$ without prior loading to $E = 0.11$ after $13.6 \text{ mg/m}^3 \times \text{h}$ loading. The lower efficiency after loading is attributed primarily to greater uncertainty in this size channel because of lower particle counts. One-way ANOVA was performed on efficiency at the three loading levels for the 15 nm particles showing no significant difference (p -value = 0.102).

Loading of particles on the impactor plate yielded minimal effects (4% to 6% difference) at the largest particle diameters ($>300 \text{ nm}$), where particle bounce had greater potential to affect the performance of the subsequent diffusion stage in the NRD sampler. Bounce of particles larger than 300 nm from the impaction plate would cause particles with substantially greater mass than nanoparticles to pass through the impactor and collect on the diffusion screens. This phenomenon would result in a positive sampling bias. The cutoff diameter of the impactor was not substantially shifted after loading ($d_{50} = 265 \text{ nm}$ for $13.6 \text{ mg/m}^3 \times \text{h}$ loading and 275 nm for $21.5 \text{ mg/m}^3 \times \text{h}$ loading). The test dust used in the loading tests contained considerable mass (10 μm volume median diameter) larger than the d_{50} of the cyclone of 4 μm , which passed through the cyclone and contributed to the loading of the impaction plate. This indicates that the impaction substrate can handle worst-case particle loadings without experiencing substantial shifts in the way that the impactor performs.

Lee et al.(32) evaluated the performance of a greased metal plate in a single-stage, single-orifice impactor by loading up to $17 \text{ mg/m}^3 \times \text{h}$ polydisperse glass beads. They observed that at this loading there was minimum particle bounce and re-entrainment. The collection efficiency for particles larger than d_{50} remained high (95%) and constant, although the collection efficiency curve was shifted and the d_{50} decreased from 5.26 to 4.36 μm . The discrepancy in the results of Lee et al.(32) and the ones of the present study may be due to several factors. The acceleration nozzle of Lee's single-stage impactor was rectangular ($W = 0.15 \text{ cm}$ and $L = 5.59 \text{ cm}$), with a substantially larger cutpoint (5.26 μm) than the impactor developed for the NRD sampler. Additionally, the loading tests of Lee et al. were performed with glass spheres with size ranging between 3 and 10 μm , very different from the irregular surfaces of the dust particles used in this study's loading tests.(33) Particles with uneven surfaces may experience increased adhesion to the greased impaction surface, making them less prone than spheres to the formation of a cone in the center of the impaction plate. The formation of a cone of deposited particles on the impaction surface has been found to shift the efficiency curve to smaller diameter particles.(34, 35) However, visual inspection confirmed the absence of these cones after the loading tests performed on the impaction plate of the NRD sampler.

Effective Deposition to the Screens of the NRD Sampler

The direct measurement of effective deposition of particles to the eight screens of the NRD sampler is shown in Figure 4 (open symbols). Deposition was lowest ($6\% \pm 2\%$) for 500 nm particles, where the impactor efficiency was at its maximum, and gradually increased with decreasing particle size. This figure shows that the deposition to the screens was in agreement with the NPM sampling criterion (solid line), within uncertainty, for all points with the exception of the 200 and 500 nm particles where it matched within $<4\%$. This means that particles deposited on the screens can be analyzed to determine the concentration of nanoparticles that would deposit in the respiratory system.

Few examples of samplers with efficiencies matching respiratory deposition can be found in the literature. Of note is the size-selective inlet designed to mimic a modified ICRP lung deposition fraction for particles smaller than 1 μm developed by Kuo et al.(36) The inlet was designed to remove large ($>1 \mu\text{m}$) and small ($<0.02 \mu\text{m}$) particles and produce a resulting aerosol that simulates only the fraction *reaching* the ciliated regions of the lungs. No collection substrate following the inlet was developed, and rationale for the target curve that they used was not provided. Koehler et al.(37) used polyurethane foam (PUF) as a selector and collector for particles to mimic total aerosol deposition in the respiratory tract. This PUF sampler follows the ICRP total respiratory deposition model. The PUF sampler provides a more physiologically relevant estimate of aerosol hazard than samplers that estimate aerosol aspiration fractions;(37) however, the PUF sampler is not specific to nanoparticles.

The NRD sampler presents an advantage over samplers traditionally used to collect particles in workplaces. Inhalable, thoracic and respirable particulate matter samplers are designed to collect particulate matter that penetrates to a specific region of the respiratory tract.(15, 38) These samplers cannot be used for accurate estimation of particulate matter deposited in the respiratory tract because not all particles that are aspirated deposit.(37) In contrast, particles

collected to the deposition stage of the NRD sampler represent the fraction of particulate matter smaller than 300 nm that deposits in the respiratory system. This deposited fraction provides a more reliable dose estimate and may better reflect adverse health effects related to nanoparticle aerosol inhalation.(39) This is particularly true for particles smaller than 300 nm as their deposition can occur anywhere in the respiratory tract.(19)

Unlike respirable and inhalable particles, there is currently no available consensus on a sampling criterion for nanoparticles. In the absence of a consensus, the NPM criterion was developed as target efficiency for the NRD sampler, following the best available deposition curve for nanoparticles in the respiratory tract and agreeing with experimental lung deposition studies. The NRD sampler can be modified in the future to follow a different deposition curve, should a different international standard than the one proposed here ultimately be adopted. The impaction stage can be modified (using impaction theory) to adjust for the size fraction penetrating into the diffusion stage, and the number and mesh size of the screens in the diffusion stage can be modified (using filtration theory) to match a different deposition curve.

The NRD sampler has some limitations that constrain its intended use to the estimation of personal exposures to airborne metal and metal-oxide nanoparticles. Sections of the nylon mesh screens can be analyzed with scanning electron microscopes for sizing, counting and assessing chemical composition of the particles collected on the nylon fibers. However, a comprehensive analysis of the particulate collected with the NRD sampler at this time requires digestion of the nylon media and recovery of the particles, which we are working on for metallic nanoparticles. The collection efficiency of the NRD sampler has been characterized for spherical and agglomerate metal particles. Its performance for fibrous particles such as carbon nanotubes is unknown. Fibrous particles may remain trapped in the impaction stage and depending on their orientation in the airstream their deposition on the diffusion stage of the NRD sampler may not reflect the NPM criterion for deposition in the respiratory tract.

The lightweight, personal NRD sampler was developed to selectively collect particles smaller than 300 nm similar to their typical deposition in the respiratory tract. The pressure drop of the NRD sampler is sufficiently low to permit its operation with conventional, belt-mounted sampling pumps. With chemical analysis of the diffusion media, the NRD sampler can be used to directly assess exposures to nanoparticles of a specific composition apart from other airborne particles.

Future work will include field tests of the NRD sampler to distinguish nanoparticles apart from background aerosols. Practical considerations will be assessed, including sample duration, frequency of impaction plate cleaning and regreasing, the effects of tipping the cyclone-based sampler, and increases of pressure drop across the diffusion stage with mass loading. In addition, analytical techniques require further elaboration, including nylon mesh digestion and detection limit determination.

Supplementary Material

Refer to Web version on PubMed Central for supplementary material.

Acknowledgments

We acknowledge the financial support from a pilot project research training grant from the Heartland Center for Occupational Health and Safety at the University of Iowa. The Heartland Center, an Education and Research Center, is supported by Training Grant No. T42OH008491 from the Centers for Disease Control and Prevention/ National Institute for Occupational Safety and Health. Financial support was also provided by National Institute for Occupational Safety and Health (1R21OH009920).

References

1. Hansen SF, Michelson ES, Kamper A, Borling P, Stuer-Lauridsen F, Baun A. Categorization framework to aid exposure assessment of nanomaterials in consumer products. *Ecotoxicology*. 2008; 17:438–447. [PubMed: 18454314]
2. Papp T, Schiffmann D, Weiss D, Castranova V, Vallyathan V, Rahman Q. Human health implications of nanomaterial exposure. *Nanotoxicology*. 2008; 2(1):9–27.
3. Oberdörster G, Ferin J, Lenhert BE. Correlation between particle size, in vivo particle persistence, and lung injury *Environ. Health Perspect*. 1994; 102(suppl 5):173–179.
4. Grassian VH, Adamcakova-Dodd A, Pettibone JM, O'Shaughnessy PT, Thorne PS. Inflammatory response of mice to manufactured titanium dioxide nanoparticles: Comparison of size effects through different exposure routes. *Nanotoxicology*. 2007; 1(3):211–226.
5. Oberdörster G, Sharp Z, Atudorei V, Elder A, Gelein R, Lunts A, Cox C. Extrapulmonary translocation of ultrafine carbon particles following whole-body inhalation exposure of rats. *J Toxicol Environ Health, Part A*. 2002; 65:1531–1543. [PubMed: 12396867]
6. Oberdörster G, Sharp Z, Atudorei V, Elder A, Gelein R, Kreyling W, Cox C. Translocation of inhaled ultrafine particles to the brain. *Inhalation Toxicol*. 2004; 16:437–445.
7. NIOSH. [accessed 7/11/2011] Current Intelligence Bulletin 63: Occupational Exposure to Titanium Dioxide. <http://www.cdc.gov/niosh/docs/2011-160/pdfs/2011-160.pdf>. 2011
8. Vincent, JH. Particle Size-Selective Sampling for Particulate Air Contaminants. American Conference of Governmental Industrial Hygienists (ACGIH); Cincinnati, OH. 1999;
9. American Conference of Governmental Industrial Hygienists (ACGIH). TLVs and BEIs Based on the Documentation of the Threshold Limit Values for Chemical Substances and Physical Agents and Biological Exposure Indices. ACGIH; Cincinnati, OH: 2010.
10. Johnson DL, Esmen NA. Method-induced misclassification for a respirable dust sampled using ISO/ACGIH/CEN criteria. *Ann Occup Hyg*. 2004; 48:13–20. [PubMed: 14718341]
11. Yeh HC, Cheng YS, Orman MM. Evaluation of various types of wire screens as diffusion battery cells. *J Colloid Interface Sci*. 1982; 86(1):12–16.
12. Kleinstreuer C, Zhang Z, Donohue JF. Targeted drug-aerosol delivery in the human respiratory system. *Annu Rev Biomed Eng*. 2008; 10:195–220. [PubMed: 18412536]
13. Grohse, PM. Trace element analysis of airborne particles by atomic absorption spectroscopy, inductively coupled plasma-atomic emission spectroscopy, and inductively coupled plasma-mass spectrometry. In: Landsberger, S.; Creatchman, M., editors. *Environmental Analysis of Airborne Particles. Advances in Environmental, Industrial and Process Control Technologies*. Vol. 1. Gordon and Breach Science Publishers; The Netherlands, Amsterdam: 1999. p. 1-65.
14. Gorbunov B, Priest ND, Muir RB, Jackson PR, Gnewuch H. A novel size-selective airborne particle size fractionating instrument for health risk evaluation. *Ann Occup Hyg*. 2009; 53(3):225–237. [PubMed: 19279163]
15. Soderholm SC, McCawley MA. Should dust samplers mimic human lung deposition? *Appl Occup Environ Hyg*. 1990; 5:829–35.
16. Heyder J, Gebhart J, Rudolf G, Schiller CF, Stahlhofen W. Deposition of particles in the human respiratory tract in the size range 0.005–15 μm . *J Aerosol Sci*. 1986; 17:811–825.

17. Kim CS, Hu SC. Regional deposition of inhaled particles in human lungs: Comparison between men and women. *J Appl Physiol*. 1998; 84:1834–1844. [PubMed: 9609774]
18. Kim CS, Jaques PA. Respiratory dose of inhaled ultrafine particles in healthy adults. *Philos Trans R Soc London*. 2000; A358:2693–2705.
19. International Commission on Radiological Protection (ICRP). Human Respiratory Tract Model for Radiological Protection. Elsevier Science, Ltd; Oxford, U.K: 1994. Publication 66
20. Cheng YS, Yeh HC. Theory of a screen-type diffusion battery. *J Aerosol Sci*. 1980; 11:313–320.
21. Peters TM, Chein H, Lundgren DA. Comparison and combination of aerosol size distributions measured with a low pressure impactor, differential mobility particle sizer, electrical aerosol analyzer, and aerodynamic particle sizer *Aerosol Sci. Technol*. 1993; 19:396–405.
22. Hinds, WC. *Aerosol Technology: Properties, Behavior, And Measurements of Airborne Particles*. John Wiley & Sons, Inc; New York, NY: 1999.
23. Tolocka MP, Tseng PT, Wiener RW. Optimization of the wash-off method for measuring aerosol concentrations *Aerosol Sci. Technol*. 2001; 34(5):416–421.
24. Furuuchi M, Eryu K, Nagura M, Mitsuhiko H, Kato T, Tajima N, Otani Y. Development and performance evaluation of air sampler with inertial filter for nanoparticle sampling *Aerosol Air Qual. Res*. 2010; 10:185–192.
25. Marple, VA.; Olson, BA.; Rubow, KL. Inertial, gravitational, centrifugal, and thermal collection techniques. In: Baron, PA.; Willeke, K., editors. *Aerosol Measurement: Principles, Techniques, And Applications*. 2. John Wiley and Sons, Inc; New York, NY: 2001. p. 229-260.
26. Hering SV, Flagan RC, Friedlander SK. Design and evaluation of new low-pressure impactor, 1. *Environ Sci Technol*. 1978; 12(6):667–673.
27. Hering, SV.; Marple, V. Low pressure and micro-orifice impactors. In: Lodge, JP.; Chan, TL., editors. *Cascade Impactors*. American Industrial Hygiene Association (AIHA); Akron, OH: 1986.
28. Hillamo RE, Kauppinen EI. On the performance of the Berner low pressure impactor. *Aerosol Sci Technol*. 1991; 14:33–47.
29. Marple VA, Rubow KL, Behm SM. A microorifice uniform deposit impactor (MOUDI): description calibration and use. *Aerosol Sci Technol*. 1991; 14(4):434–446.
30. Hering SV, Friedlander SK, Collins JJ, Richards LW. Design and evaluation of a new low-pressure impactor, 2. *Environ Sci Technol*. 1979; 13(2):184–188.
31. Misra C, Singh M, Shen S, Sioutas C, Hall PM. Development and evaluation of a personal cascade impactor sampler (PCIS). *Aerosol Sci*. 2002; 33:1027–1047.
32. Lee SJ, Demokritou P, Koutrakis P. Performance evaluation of commonly used impaction substrates under various loading conditions. *J Aerosol Sci*. 2005; 36(7):881–895.
33. Vlasenko A, Sjorgen S, Weingartner E, Gaggeler HW, Ammann M. Generation of submicron arizona test dust aerosol: chemical and hygroscopic properties *Aerosol Sci. Technol*. 2005; 39:452–460.
34. Vanderpool RW, Peters TM, Natarajan S, Gemmill DB, Wiener RW. Evaluation of the loading characteristics of the EPA WINS PM2.5 separator. *Aerosol Sci Technol*. 2001; 34:444–456.
35. Peters, TM.; Volckens, J.; Hering, SV. *Impactors, Cyclones, And Other Particle Collectors: A Monograph of the ACGIH® Air Sampling Instruments, Committee publication #AS113*. American Conference of Governmental Industrial Hygienists; Cincinnati, OH. 2009;
36. Kuo YM, Huang SH, Shih TS, Chen CC, Weng YM, Lin WY. Development of a size-selective inlet-simulating ICRP lung deposition fraction. *Aerosol Sci Technol*. 2005; 39:437–443.10.1080/027868290956602
37. Koehler KA, Clark P, Volckens J. Development of a sampler for total aerosol deposition in the human respiratory tract. *Ann Occup Hyg*. 2009; 53(7):731–738. [PubMed: 19638392]
38. Soderholm SC. Proposed international conventions for particle size-selective sampling. *Ann Occup Hyg*. 1989; 33:301–320. [PubMed: 2802448]
39. Esmen NA, Johnson DL. The variability of delivered dose of aerosols with the same respirable concentration but different size distributions. *Ann Occup Hyg*. 2002; 46:401–7. [PubMed: 12176709]

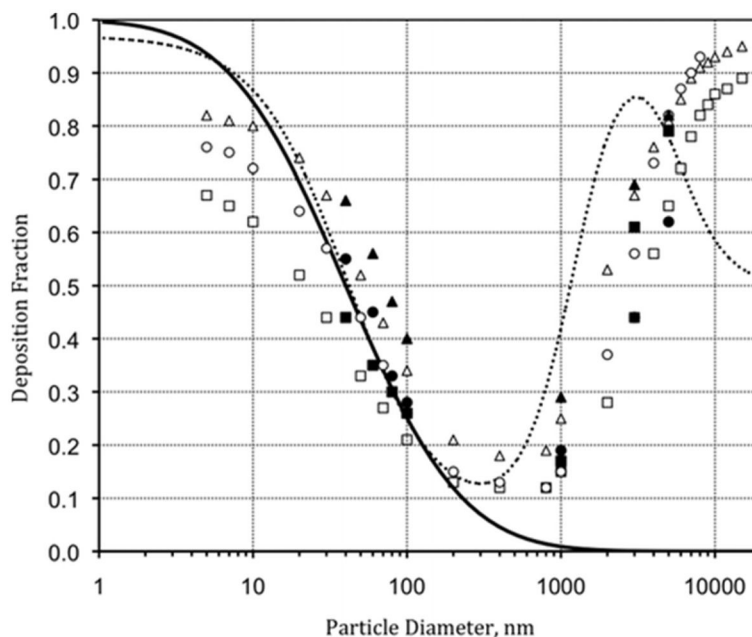


Figure 1.

Total deposition fraction versus particle diameter (aerodynamic). — is the NPM criterion; is deposition in all regions of the respiratory tract as defined by the ICRP.(19) All other symbols are deposition fraction in the normal lung at FRC=3000 mL for controlled breathing patterns. Open symbols are data from Heyder et al. (1986): □ is $V_t = 500$ mL, $Q = 250$ mL/s; △ is $V_t = 1000$ mL, $Q = 250$ mL/s; ○ is $V_t = 1000$ mL, $Q = 500$ mL/s. Closed symbols are data of Kim and Hu (1998) and Kim and Jaques (2000): □ is $V_t = 500$ mL, $Q = 250$ mL/s; ▲ is $V_t = 1000$ mL, $Q = 250$ mL/s; ● is $V_t = 1000$ mL, $Q = 500$ mL/s. V_t = tidal breathing volume and Q = air flow rate.

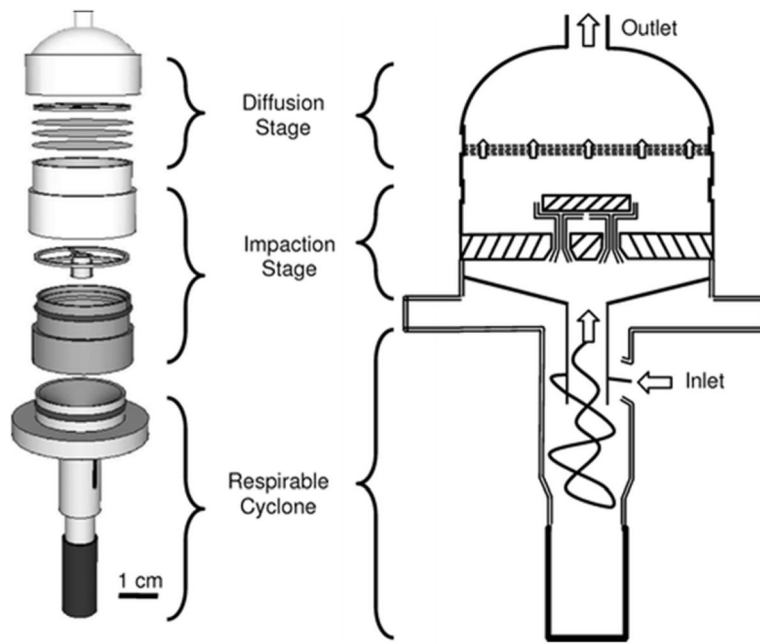


Figure 2. The components and schematic drawing with airflow paths of the NRD sampler.

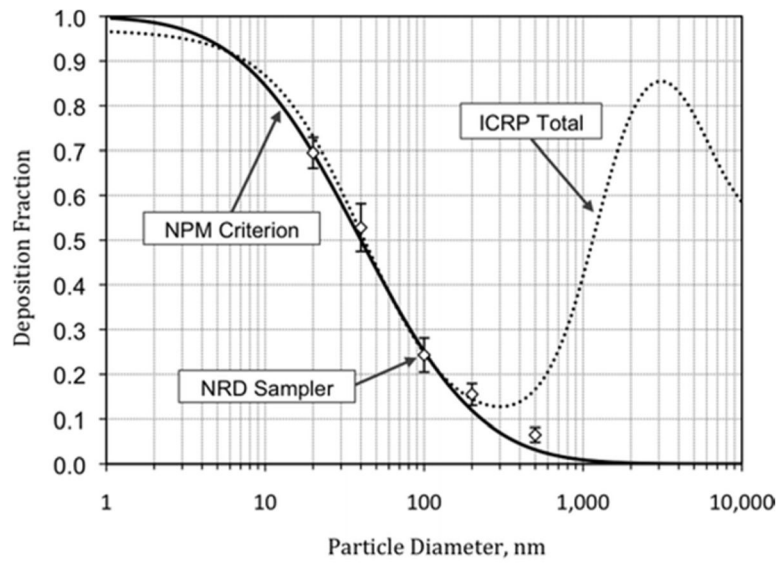


Figure 4. NPM sampling criterion, ICRP total respiratory deposition(19) and effective deposition on the diffusion stage of the NRD sampler.

Table 1Physical Characteristics, Flow Parameters and Experimental Results of the Impaction Stage^a

Physical Characteristics	
<i>W</i> (cm)	0.053
<i>L</i> (cm)	0.135
<i>S/W</i>	1.9
Flow Parameters	
<i>Re</i>	2212
<i>V</i> (cm/sec)	6295
Experimental Results	
<i>d</i> ₅₀ (μm)	0.295
Stk ₅₀	0.47
σ	1.53
<i>P</i> (kPa)	2.49

^aNote: *W*, nozzle width; *L*, nozzle lengths; *S*, impaction plate-to-nozzle distance; *Re*, Reynolds number; *V*, nozzle air velocity; *d*₅₀, 50% cutpoint; Stk₅₀, square root of Stokes number at 50% collection efficiency; σ, collection efficiency curve sharpness; *P*, pressure drop; Stokes number at the 50% cut-off diameter is calculated as $Stk_{50} = (4\rho_p Q d_p^2 C_C) / (9\pi\eta\mu W^3)$, where *d*_p is the mobility equivalent particle diameter, and *C*_C is Cunningham slip correction factor.

Table 2

Effects of Loading on Collection Efficiency of the Impaction Stage

particle diameter [nm]	prior impactor loading [$\text{mg}/\text{m}^3 \times \text{h}$]		
	0	13.6	21.5
	collection efficiency (stdev)		
15	0.26 (0.08)	0.11 (0.08)	0.15 (0.06)
50	0.12 (0.02)	0.08 (0.04)	0.07 (0.02)
80	0.07 (0.01)	0.07 (0.04)	0.04 (0.01)
100	0.08 (0.03)	0.09 (0.02)	0.06 (0.02)
300	0.54 (0.02)	0.57 (0.01)	0.57 (0.08)
500	0.90 (0.03)	0.89 (0.01)	0.86 (0.07)
800	0.98 (0.02)	0.97 (0.01)	0.92 (0.08)
1000	0.99 (0.01)	0.97 (0.01)	0.93 (0.07)

Author Manuscript

Author Manuscript

Author Manuscript

Author Manuscript